Analysis and description of cyclocopter performances

Alberto Ramos Escobar
alberto.ramos.escobar@tecnico.ulisboa.pt

Instituto Superior Técnico, Universidade de Lisboa, Portugal

November 2021

Abstract

Following the growing interest in the use of drones, this research is focused on studying and analysing their performances but using a specific type of rotor: the cyclorotor. Therefore, the fundamentals of cyclocopter, which is the name that receive this type of UAV, are explained from a dimensional point of view. This objective is achieved by developing some numerical codes which allow to approximate and so, to understand the behaviour of the flow around the blades of the cyclorotor. Finally, the thrust produced and the power consumed are the most important values to obtain and so, some results are presented showing the evolution of these variables when some dimensional or aerodynamic parameters are varied.

Keywords: Cyclocopter, Unsteady Aerodynamics, Induced Velocity, Double-Multiple Streamtube.

1: Introduction

1.1 Motivation and Objectives

The tendency of using UAV (Umanned Aerial Vehicles) is increasing year after year due to the huge variety of applications in which this type of vehicles can be used. Drones can be used in areas like surveillance, meteorology, plague control, among others.

The main goal of this thesis is to describe and analyse the aerodynamic of the cyclocopter studying velocities and forces that appear on the blades and a calculation of the power consumed is then performed. The hover case is first analysed and next, the forward motion. Moreover, three computacional models will be created using Matlab (two for hover and one for forward) and validated with experimental values obtained from different researches and like this, the general operation of the cyclocopter will be able to be represented.

1.2 General Concepts

A cyclorotor or cyclocopter is a rotating-wing system where the span of the blades runs parallel to the axis of its rotation. In this type of aircraft, the pitch angle of each blade is varied cyclically by mechanical means such that each blade experiences positive geometric angles of attack at both the top and bottom halves of its circular trajectory. The variation of the amplitude and phase of the cyclic blade pitch is used to change the magnitude and direction of the net thrust vector (T_{Res}) produced by the cyclorotor. This resultant thrust can be decomposed into lift and forward thrust which are shown in figure 1.1.

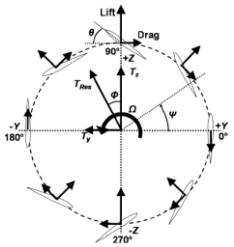

Figure 1.1: Forces in each azimuthal position [1]

1.3 Cyclocopter Blade Pitching Mechanism

This mechanism is necessary to allow the cyclorotor to be used on a flying vehicle. It is passive mechanism consisting mainly of two bearings, one inserted in the other, and the linkages are connected to the offset ring which is installed around the second bearing. So, if the connection between the axis of rotation and the mechanism is direct, the only losses that appear are due to the friction of the moving components. The goal is to try to find an analytical model in order to be able to calculate the pitch angle θ in every azimuthal position Ψ of the blades. According to reference [2], the solution equation is the following one:

$$\theta(t) = \frac{\pi}{2} - sin^{-1}\left[\frac{L_2}{a}cos(\Psi+\phi)\right] - cos^{-1}\left(\frac{a^2+d^2-L_3^2}{2aL_4}\right) \quad (1.1)$$

where all lengths and angles are shown in the following figure 1.2:

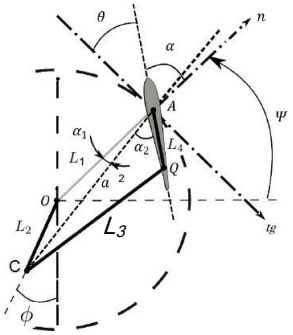

Figure 1.2: Schematic for pitching mechanism [2]

2: Aerodynamic Analysis

2.1 Reduced Frequency (k)

Like in helicopter performances, the design of new UAVs has improved due to the ability to predict accurately the aerodynamic behaviour of the rotor (cyclorotor) in all the operational envelope. However, the major difficulty is to describe the unsteady aerodynamic effects that appear, especially in high speed forward flight and during maneuvers with the aim to approximate their impact on the airloads and the performances. In order to characterize these unsteady effects, the reduced frequency (k) is the most important parameter which allows the definition of a degree of unsteadiness of the problem. The definition of this parameter in terms of the airfoil semi-chord $b=c/2$ is: $k = \frac{\omega b}{V} = \frac{\omega c}{2V}$ where ω is the angular frequency of the problem, c is the airfoil and V is the flow velocity.

2.2 Unsteady Models

All the information which is going to be presented in this section is obtained from reference [3].

2.2.1 Theodorsen's Theory

Theodorsen's model gives a solution to the unsteady airloads on a 2-D harmonically oscillated airfoil in inviscid, incompressible flow and subject to small disturbance assumptions. However, this problem is not trivial but for simple harmonic motion, Theodorsen gives a simple solution in terms of lift and pitching moment coefficients if a particular movement is forced like considering harmonic pitch oscillations, where the forcing is given by $\alpha = \bar{\alpha}e^{i\omega t}$ and the pitch rate by $\dot{\alpha} = i\omega\bar{\alpha}e^{i\omega t}$:

$$C_l = 2\pi[F(1+ik) + G(i-k)]\bar{\alpha}e^{i\omega t} + \pi k\left(i - \frac{k}{2}\right)\bar{\alpha}e^{i\omega t}$$

$$C_m = \frac{\pi k}{2}\left(\frac{3}{8}k - i\right)\bar{\alpha}e^{i\omega t}$$

where α is the angle of attack, t is the time step, k is the reduced frequency and the complex function $C(k) = F(k) + iG(k)$ is

known as Theodorsen's function and it is used to take into account the effects of the shed wake on the unsteady airloads.

2.2.2 Indicial Response Method

This method is very useful if the indicial aerodynamic response can be determined. Then, it is possible to find the unsteady aerodynamics forces and moments in the time domain as a result of arbitrary variations in angle of attack and/or inflow velocity by using Duhamel superposition. The time-varying value of the lift coefficient can be expressed in terms of the Duhamel integral as:

$$C_l(s) = C_{l\alpha}[\alpha(s_0)\phi(s) + \int_{s_0}^{s} \frac{d\alpha}{ds}(\sigma)\phi(s-\sigma)d\sigma] = C_{l\alpha}\alpha_e(s)$$

where ϕ(s) is the indicial response, also called the Wagner function, to an unit step input of the angle of attack and $C_{l\alpha}$ is the lift curve slope. The problem here is that the Wagner function ϕ(s) is not always known in a convenient simple analytic form. One solution to the problem is supposing that the Wagner function takes the form of a general two-term exponentially growing function:$\phi(s) = 1 - A_1 e^{-b_1 s} - A_2 e^{-b_2 s}$. Moreover, the Duhamel integral can be written in compact form as $\alpha_e(s) = \alpha(s) - X(s) - Y(s)$ where the X and Y terms are given by:

$$X(s) = X(s-\Delta s)e^{-b_1 \Delta s} + A_1 \Delta\alpha_s$$

$$Y(s) = Y(s-\Delta s)e^{-b_2 \Delta s} + A_2 \Delta\alpha_s$$

This form of X and Y terms is named as one-step recursive formulas or Algorithm D-1 and contain all the time history information of the unsteady aerodynamics and are simply updated once at each time step.

2.3 Inflow Dynamic Analysis

The goal of this section is to define different inflow models which are going to be used in order to predict and analyse the aerodynamics of the cyclocopter. First, the hover situation is going to be covered and next, the forward flight.

2.3.1 Hover Flight

The two inflow models which are going to be used in order to predict and analyse the aerodynamics of the cyclocopter in hover flight are the followings:

- Single Streamtube Model (SS) [1]: The entire rotor is immersed in a unique streamtube (figure 2.1 (a)).
- Double-Multiple Streamtube Model (DS) [4]: The rotor is divided into a number of streamtubes and the influence of the upper half of the rotor on the lower half is taken into account (figure 2.1 (b)).

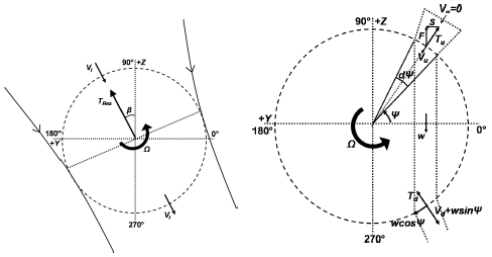

Figure 2.1: (a) Single Streamtube Inflow (b) Double-Multiple Streamtube Inflow [1]

2.3.1.1 Single Streamtube Model

The final result of the models is the blade aerodynamic loads (lift and drag). Moreover, it is necessary to make an iterative process in order to use the final solution of the problem to obtain the direction of the resultant thrust β and the inflow velocity v_i and solve again the problem with the correct values.

So, the first step is the calculation of the section angle of attack which has two components: the wind velocity $(\vec{V}_w)$ from rotor inflow and the blade velocity at the ¾ chord location $(\vec{V}_b)$ relative to the hub fixed frame. However, these velocities are needed to be expressed in the deformed frame in order to calculate the blade section loads and so, the rotation matrix T_{DU} is used.

In order to solve the aerodynamic of the cyclocopter and take into account the unsteady effects, the indicial response method explained in section 2.2.2 is going to be used. In relation to the total drag coefficient, this is given by the sum of profile C_{d0} and induced drag C_{di} components:

$$C_d = C_{d0} + C_{di}$$

The next step is to calculate the forces in the deformed frame and rotate them to the undeformed frame. Finally, the thrust produced and the power consumed are calculated.

2.3.1.2 Double-Multiple Streamtube Model

In this model, each streamtube intersects the blades' path twice, once on the upstream pass and again on the downstream pass. Therefore, the two halves of the cycle are going to be analysed separately but also take into account the interaction between them.

Upstream half of the rotor ($0 \leq \Psi \leq \pi$)

In order to define this upstream half, the next equation need to be solved:

$$4\kappa_{emp}\lambda^2 = \sigma a(1+\lambda^2)[(\theta - \phi)\cos\phi - \frac{C_d}{a}sin\phi]sin^2\Psi$$

where σ is the blade solidity, ϕ is the relative inflow angle, θ is the pitch angle and κ_{emp} is an empirical factor to take into account non-uniform flow, 3-D effects, tip losses, etc... and it is assumed to be 1.15. Therefore, the resultant velocity U_R, the relative inflow angle ϕ at the blade element and the angle of attack α are:

$$U_R = \sqrt{U_T^2 + U_P^2} \;\; ; \;\; \phi = tan^{-1}\left(\frac{U_P}{U_T}\right); \;\; \alpha = \theta - \phi$$

Finally, the far downstream velocity of the upstream half w can be obtained thanks to the following equation: $w = \frac{2v_u}{sin\Psi}$ (2.1)

Downstream half of the rotor ($\pi \leq \Psi \leq 2\pi$)

In this downstream half, the following equation need to be solved:

$$4(\lambda - \varsigma\, tan\Psi)\sqrt{\lambda^2 + \varsigma^2} =$$
$$\sigma[(1+\tau)^2 + \lambda^2][a(\theta - \phi)\cos\phi - C_d sin\phi$$

where $\varsigma = \frac{w cos\Psi}{R\Omega}$ and the values of w are given by equation 2.1 because for this downstream half, w is considered as an input condition of the flow at each streamtube defined in the upper half. Since the velocities in both up and down halves of the rotor are obtained, the next step is to determine the forces. Therefore, the total thrust produced and the power required can be obtained.

2.3.2 Forward Flight

This simplified numerical model used to approximate the forward flight is explained thanks to reference [2]. It is obtained by simple Cartesian vector analysis and the application of the Pythagorean theorem. Therefore, the equations obtained according to reference [2] are the following ones:

$$V_T = \Omega R + V_h \sin(\Psi) + V_v \cos(\Psi) \qquad (2.2)$$

$$V_N = V_h \cos(\Psi) - V_v \sin(\Psi) \qquad (2.3)$$

$$\gamma = arctan\left(\frac{V_N}{V_T}\right) \;\; ; \;\; V_R = \sqrt{V_T^2 + V_N^2} \;\; ; \;\; \theta_a = \gamma + \theta \qquad (2.4)$$

where V_T and V_N are the velocity tangential and normal components respectively, V_h and V_v are the horizontal and vertical advance velocities respectively, γ is the resultant velocity slope in relation to the tangential axis and θ_a is the angle of attack for each blade in forward motion. The different types of motion can be studied thanks to the values of V_h and V_v.

As it happened in the DS code for hover case, the lift and drag coefficients calculation follows the same procedure as well as the forces and the power consumed.

3: Hover Flight Analysis

3.1 Models Validation

The aim of this section is to show if the model can approximate and adapt well to the reality. In order to make it possible, the results obtained from the model are compared with experiments. Two subsections are going to be presented using two

different ways to vary the pitch angle: one considering a sinusoidal variation and the other with the four-linkage mechanism explained in section 1.3 and defined by equation 1.1.

3.1.1 Sinusoidal Pitch Angle Variation

The sinusoidal variation of the pitch angle along the azimuthal position is expressed by the following equation:

$$\theta = \theta_0 \sin(\Psi) \quad (2.5)$$

where θ_0 is the amplitude of the sine and so, the maximum value of the pitch angle. The experimental results used in this subsection are extracted from reference [4]. The performance parameters that define the geometry of the cyclocopter and which are used to obtain the figure 3.1 are shown in table 3.1.

Table 3.1: Geometry of cyclocopter used in figure 3.1

c(m)	R(m)	b(m)	N_b	θ_0(º)
0.15	0.4	0.8	6	15

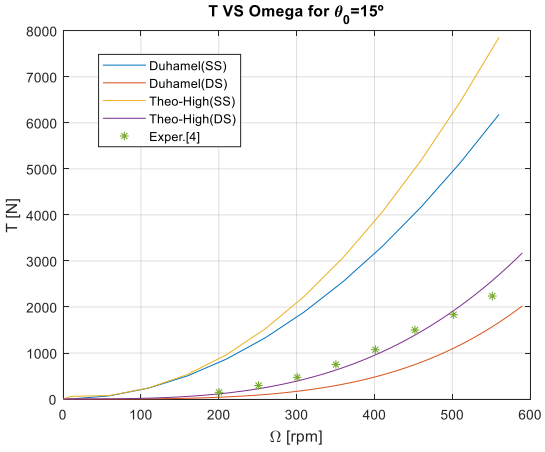

Figure 3.1: Resultant Thrust VS Rotation Speed for maximum pitch amplitude of θ_0=15º

As it can be seen in figure 3.1, the Double-Multiple Streamtube model (DS) using Theodorsen's theory with high unsteady effects is the model which adapts better to the experimental values. This conclusion allows to validate this model as the most suitable one to be used to obtain results about the performance of cyclocopters.

3.1.2 Four-bar Linkage Pitch Angle Mechanism

Since DS model with Theodorsen's theory gives the best results, this model is going to be used in this subsection but supposing three cases depending of the value of the angular frequency ω (and therefore, of the reduced frequency k): Theodorsen with steady effects, Theodorsen with low unsteady effects and Theodorsen with high unsteady effects. In addition, the table 3.2 shows the geometric parameters used to obtain the following graph.

Table 3.2: Geometry of cyclocopter used in figure 3.2

c(m)	R(m)	b(m)	N_b
0.3048	0.6096	1.2192	6

L_1(m)	L_2(m)	L_3(m)	L_4(m)	ε(º)
0.6096	0.0315	0.6134	0.075	0

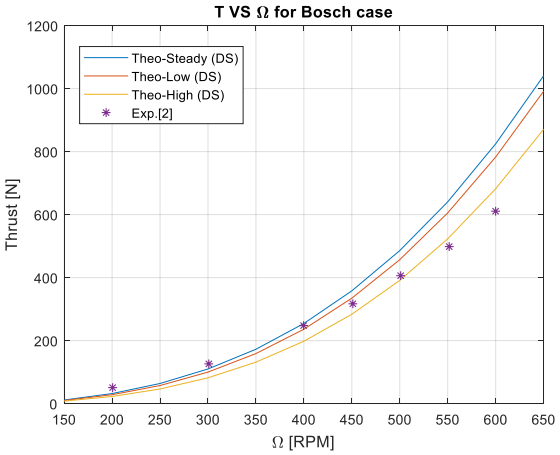

Figure 3.2: Resultant Thrust VS Rotation Speed (Bosch case)

In relation to this Bosch case (figure 3.2), the curves show that at first, the steady case adapts better to the experimental values at low rotational speeds and at higher speeds, Theodorsen's model with high unsteady effects is the best one for approximating the experimental values, which is similar to the result obtained in section 3.1.1.

3.2 Analyses of Hover Flight

3.2.1 Sinusoidal Pitch Angle Variation

In this subsection, the Double-Multiple Streamtube code (DS) is used to obtain all the results due to the fact that is a better model than

the Single Streamtube code (SS) as it was demonstrated in section 3.1.

Thrust VS Rotation speed

The geometric values used for obtaining results from this DS code were shown in table 3.1. If the radius of the blades is changed, the results obtained appear in figure 3.3.

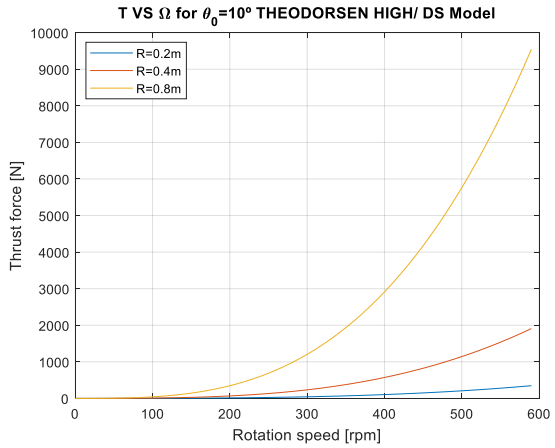

Figure 3.3: Effect of blade radius (R) on the thrust produced (Sinusoidal variation/DS inflow model)

According to figure 3.3, when the radius is increased, the thrust force produced increases as well and the slope of this increase is also higher. However, the stalling of blades has not been taken into account and it could be possible that some of these thrusts can not be achieved.

If the number of blades is now modified but maintaining the total blade area, the result is shown in figure 3.4.

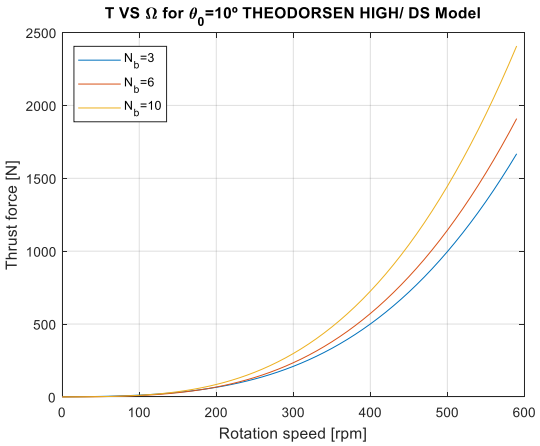

Figure 3.4: Effect of number of blades (N_b) on the thrust produced (Sinusoidal variation/DS inflow model)

Thanks to figure 3.4, it is possible to see that increasing the number of blades, the thrust produced also increases and the trend which the curves follow is more or less the same. However, the weight of the cyclocopter is higher and in some cases, it may be not a good choice to increase the number of blades since it can be heavier configuration, which may not be a desirable option.

Thrust VS Pitch Angle Amplitude

The results obtained now are the following one:

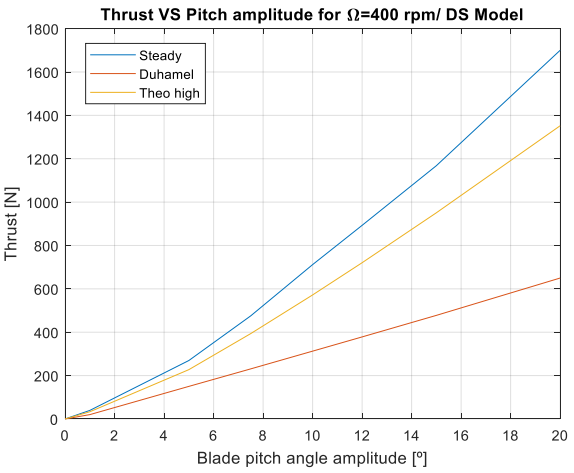

Figure 3.5: Comparison of steady and unsteady models with the pitch amplitude (Sinusoidal variation/DS inflow model)

From figure 3.5, it is possible to see that the steady case gives the highest thrust and Duhamel's model, the lowest one which is in concordance with all previous figures. Moreover, all models follow more or less a linear dependant between this two variables.

If now the rotation speed is varied, the curves obtained are shown in figure 3.6.

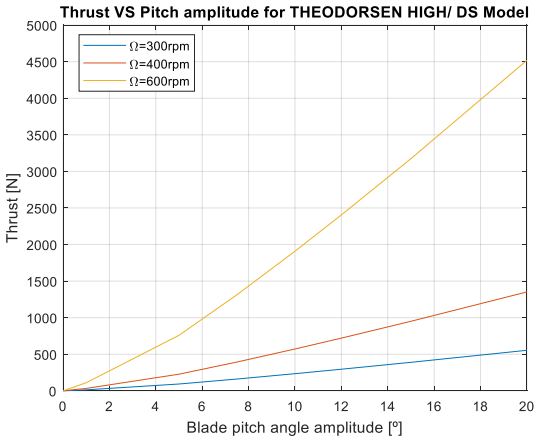

Figure 3.6: Effect of the rotation speed (Ω) on the thrust produced (Sinusoidal variation/DS inflow model)

According to figure 3.6, the thrust produced is higher when the rotation speed increases and it seems to be a linear dependence between the two variables. The problem that may appear is a structural limitation of the cyclorotor which not allow to increase more the rotation speed above a certain limit.

3.2.2 Four-bar Linkage Pitch Angle Mechanism

Thrust VS Rotation speed

The geometric values used in this subsection appear in table 3.2 and the 4-bar lengths/angle are L_1=0.4m, L_2=0.01m, L_3=0.5m, L_4=0.4m and ε=0º. In particular, the two parameters which are going to be used are the magnitude of eccentricity (L_2) and the phase angle of eccentricity (ε).

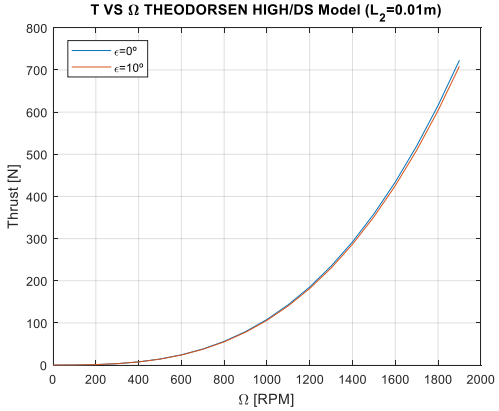

Figure 3.7: Effect of the phase angle of eccentricity (ε) on the thrust produced (4-bar mechanism/DS inflow model)

Thanks to figure 3.7, it is possible to see that the effects of changing ε on the thrust produced are not significant.

If now L_2 is varied:

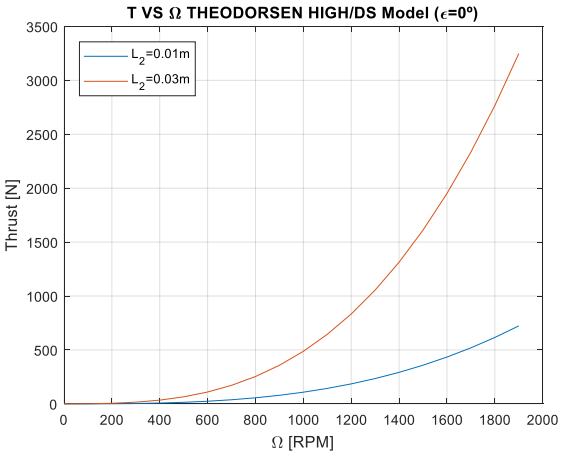

Figure 3.8: Effect of the magnitude of eccentricity (L_2) on the thrust produced (4-bar mechanism/DS inflow model)

Figure 3.8 demonstrates that increasing L_2, the thrust produced also increases.

Thrust VS Pitch Angle Amplitude

These graphs are represented in the last subsection (Thrust VS Rotation speed) when the four-bar linkage mechanism parameters are varied because this causes that the pitch angle amplitude changes. The problem here is that there is not a direct relation between the pitch amplitude and the variation of it like it occurred when a sinusoidal variation was considered. So, obtaining these graphs is not so easy and figures 3.7 and 3.8 are used to show this relation knowning that:

- Increasing L_2, the pitch amplitude is higher when the other lengths/angles remain fixed.

- The pitch amplitude does not change too much when ε is varied.

4: Forward Flight Analysis

4.1 Model Validation

The simplified numerical model used to approximate the forward flight is explained in section 2.3.2 acording to reference [2] and the

validation of the model is done comparing the variation of the angle of attack showed also in reference [2] with the variation obtained thanks to the code for hover case and the two types of movement (forward and backward). The parameters which have been used appear in table 4.1.

Table 4.1: Geometry of cyclocopter used in Figure 4.1

c(m)	R(m)	b(m)	N_b	
0.3	0.8	1.6	6	
L_1(m)	L_2(m)	L_3(m)	L_4(m)	ε(º)
0.8	0.04	0.8041	0.09	10

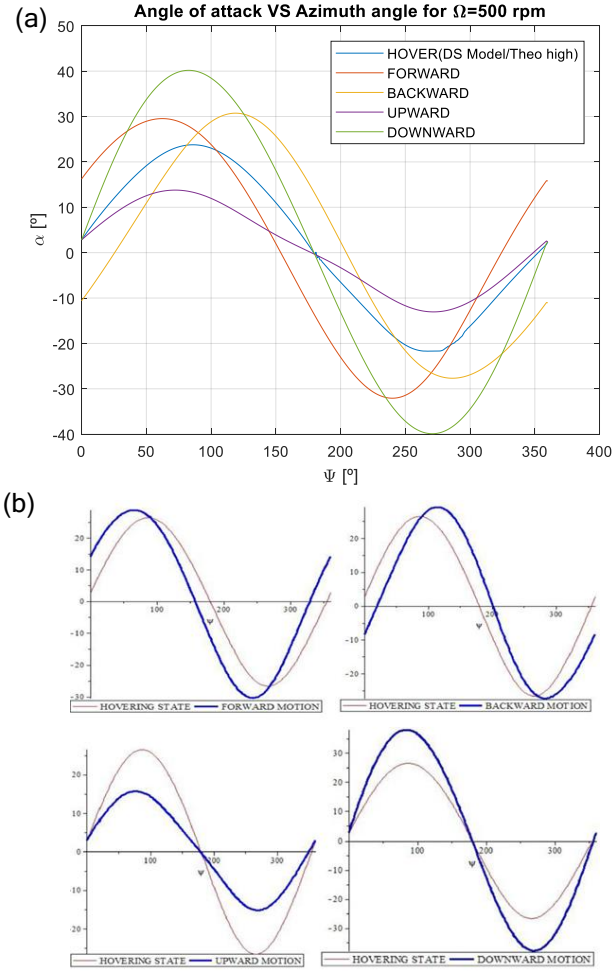

Figure 4.1: Angle of attack variation for hover, forward, backward, upward and downward performances with rotation speed of (a) 500rpm and (b) experiments from [2]

According to figure 4.1, the agreement between the model and experiments from [2] is very good.

4.2 Analyses of Forward Flight

The parameters used to obtain all the graphs which are going to be presented in this section appear in table 4.1. The first result is the variation of thrust and power with the rotation speed:

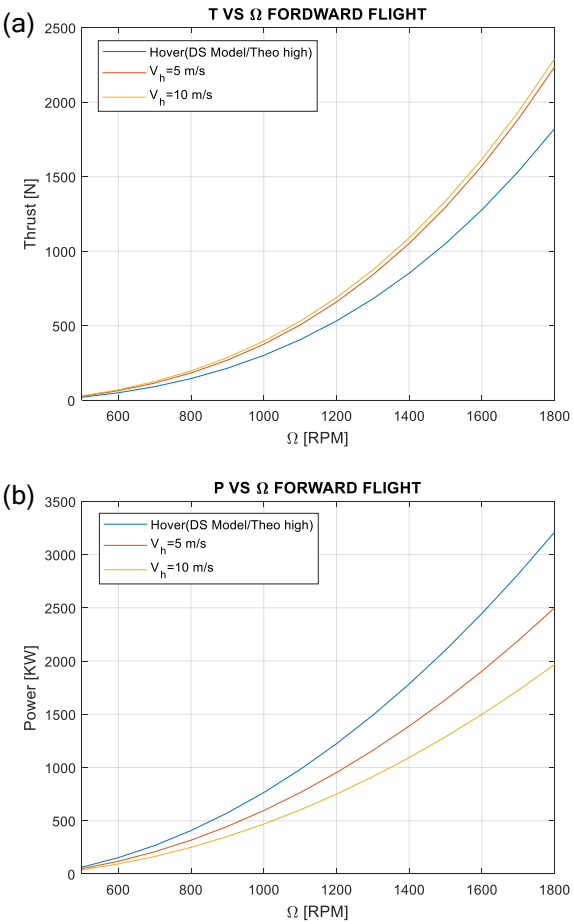

Figure 4.2: Variation of (a) thrust and (b) power with the rotation speed (Forward flight)

According to figure 4.2, increasing the forward velocity (V_h), the thrust produced increases and the power consumed decreases. Moreover, in comparison to hover case, the thrust is higher and the power is lower for this forward velocities.

Another result which may be interesting to show is the relation between the power consumed and the advance velocity. In order to do this, it is necessary to fix two parameters between these three: thrust, rotation speed or pitch angle variation. In this research, the thrust

is going to be fixed and the showed graphs are going to be obtained fixing one of the other two and varying the other one.

- FIRST CASE: Thrust and pitch angle variation fixed/ Rotation speed variable.

The result obtained is represented in figure 4.3 in which each marked point shows the necessary rotation speed to achieve this thrust.

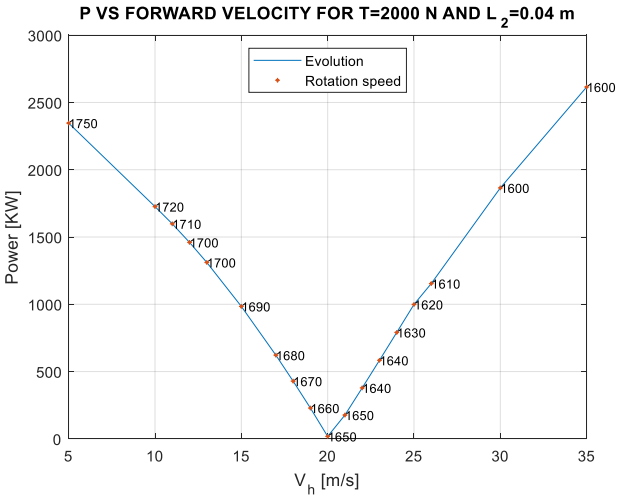

Figure 4.3: Variation of power with the advance velocity fixing thrust and pitch angle variation

Thanks to figure 4.3, it is possible to see that the power consumed is decreasing with the forward velocity until it reaches a minimum and from this point, the power starts to increase. Moreover, it is possible to see that the rotation speed is always decreasing when the advance velocity increases.

If now the pitch angle variation is fixed but with different values, the result appears in figure 4.4.

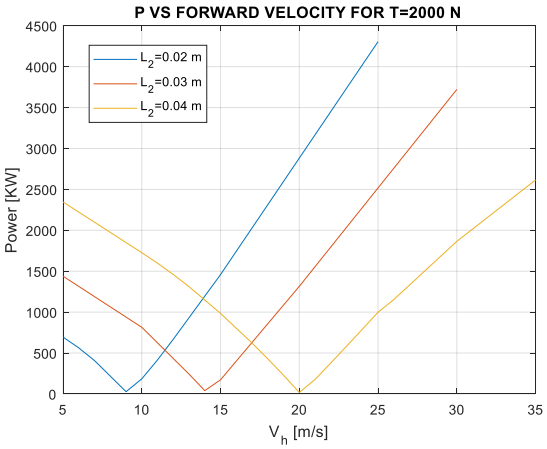

Figure 4.4: Variation of power with the advance velocity fixing thrust for different pitch angle variations

According to figure 4.4, the change in the pitch angle variation is done varying the length L_2 whose relation with the maximum pitch angle was determined in subsection 3.2.2 (increasing L_2 increases the maximum pitch angle). Therefore, the forward velocity in which the power is minimum is higher when the length L_2 increases.

- SECOND CASE: Thrust and rotation speed fixed/ Pitch angle variation variable.

This second case is represented in figure 4.5 in which each marked point shows the value of the length L_2 which is necessary to define in order to achieve the fixed thrust.

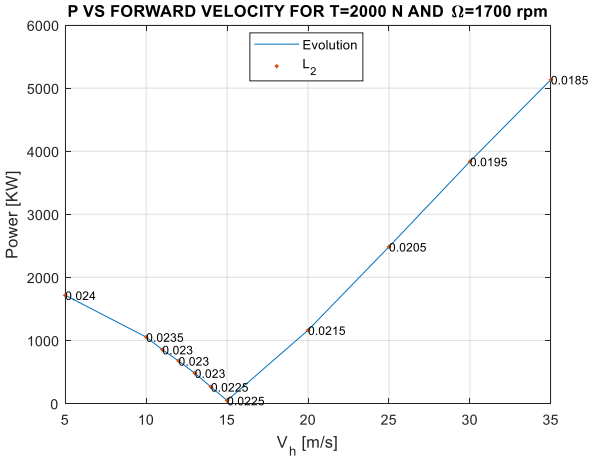

Figure 4.5: Variation of power with the advance velocity fixing thrust and rotation speed

The relation between the power and the advance velocity in this new case remains the

same as the first case because the power is decreasing until a minimum value and from this point, it starts to increase. Moreover, the length L_2 has also the same tendence as the rotation speed in case one, as the forward velocity is increasing, this length is always decreasing.

Varying now the fixed rotation speed, the result appears in the following figure 4.6:

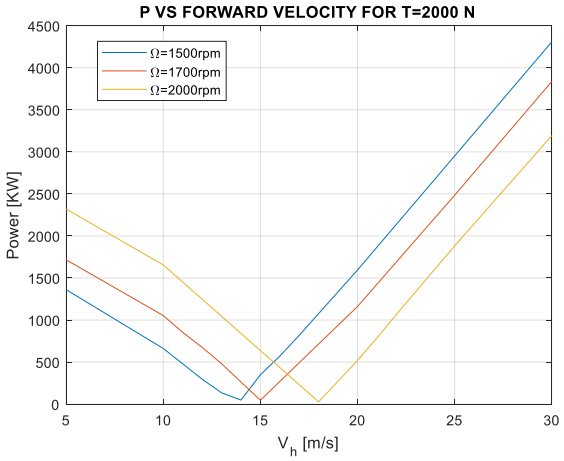

Figure 4.6: Variation of power with the advance velocity fixing thrust for different rotation speeds

Thanks to figure 4.6, it is possible to see that the forward velocity in which the power consumed is minimum is higher when the fixed rotation speed increases, occurring something similar to the previous case with the length L_2.

4: Conclusion

The main goal of this research was to study, analyse and explain the basic fundamentals about cyclocopters. Thanks to the models presented and the numerical codes developed, their performances have been able to be approximated.

The Double-multiple Streamtube (DS) code could be validated using some experimental values from references [2] and [4]. Moreover, this DS code with highly unsteady Theodorsen's model was proved to be the best model because it is the one which is best suited to the experiments.

Thanks to the results obtained using this best model, some conclusions have been able to be extracted about the behaviour of cyclocopter for hover situation and forward flight.

Finally, some future works can be done in order to continue with this research:

- Restricting the results shown in the research considering the onset of the blades stalling as well as due to the weight of the cyclorotor,

- Calculating the interaction between cyclorotors in the same aircraft as well as being possible to control the thrust module and direction of them in order to do the required performance.

- Analysing the effect of change the blade profile as well as using high-lift devices like flaps during some performances.

- As the forward flight is analysed using a simplified model, some of the results obtained need to be reviewed, maybe developing a more accurate model.

Bibliography

[1] M.Benedict. *Fundamental Understanding of the Cycloidal-Rotor Concept for Micro Air Vehicle Applications*. PhD thesis, Department of Aerospace Enginee- ring,University of Maryland, 2010.

[2] J.Monteiro, J. C.Pascoa, and C.Xisto. *Analytical modeling of a cyclorotor in forward flight*. SAE International, 2013. DOI:10.4271/2013-01-2271.

[3] J.Leishman. *Principles of Helicopter Aerodynamics*. CAMBRIDGE UNIVERITY PRESS, 1st edition,2000. ISBN:0-521-52396-6.

[4] C.Yun, I.Park, H.Lee, J.Jung, I.Hwang, S.Kim, and S.Jung. *A New VTOL UAV Cyclocopter with Cycloidal Blades System*. Proceeddings of the 60th Amercian Helicopter Society Annual Forum, Baltimore, June, 2004.